Influence of Pb doping on the electrical transport properties of BiCuSeO

Lin Pan, David Bérardan, Lidong Zhao, Céline Barreteau, and Nita Dragoe

Citation: Applied Physics Letters **102**, 023902 (2013); doi: 10.1063/1.4775593
View online: http://dx.doi.org/10.1063/1.4775593
View Table of Contents: http://scitation.aip.org/content/aip/journal/apl/102/2?ver=pdfcov
Published by the AIP Publishing

Influence of Pb doping on the electrical transport properties of BiCuSeO

Lin Pan,[a] David Bérardan, Lidong Zhao, Céline Barreteau, and Nita Dragoe
Institut de Chimie Moléculaire et des Matériaux d'Orsay, Univ. Paris-Sud, UMR 8182, Orsay F-91405, France and CNRS, Orsay F-91405, France

(Received 13 November 2012; accepted 18 December 2012; published online 14 January 2013)

The effect of Pb doping on the thermoelectric properties of *p*-type BiCuSeO from 25 K to 873 K has been studied. The electrical resistivity and Seebeck coefficient of $Bi_{1-x}Pb_xCuSeO$ both decreased monotonically in all temperature range with increasing Pb content due to the increased carrier concentration. The power factor of $Bi_{1-x}Pb_xCuSeO$ ($x = 0.03$) reaches 5.3 μW cm^{-1} K^{-2} at 873 K. The influence of Pb^{2+} doping on the electronic structure is the same as the one obtained with Sr^{2+}, however, the decrease of the holes mobility is reduced as compared to Sr^{2+} doping, which could be beneficial to the thermoelectric performances. © *2013 American Institute of Physics*. [http://dx.doi.org/10.1063/1.4775593]

Thermoelectric (TE) effects enable direct conversion between thermal and electrical energy and provide an alternative route for power generation and refrigeration.[1,2] The TE conversion efficiency of TE materials is an increasing function of the dimensionless figure of merit $ZT = (S^2T)/(\rho\kappa)$, where S, ρ, κ, and T are Seebeck coefficient, electrical resistivity, thermal conductivity, and absolute temperature, respectively.

Recently, compared with polycrystalline oxide systems such as *p*-type $Ca_3Co_4O_9$ ($ZT \sim 0.2$ at 973 K),[3] or *n*-type $SrTiO_3$ ($ZT \sim 0.35$ at 1273 K),[4] ZnO ($ZT \sim 0.4$ at 1273 K)[5] or In_2O_3 ($ZT \sim 0.45$ at 1273 K),[6,7] p-type BiCuSeO, a layered oxychalcogenide composed of conductive $(Cu_2Se_2)^{2-}$ layers alternately stacked with insulating $(Bi_2O_2)^{2+}$ layers,[8] has attracted attention for its promising thermoelectric performances which mainly originated from its low thermal conductivity (0.46 W m^{-1} K^{-1} at 873 K) coupled to a moderate power factor S^2/ρ.[9] This very low thermal conductivity, much lower than the one observed in other state of the art thermoelectric materials in the same temperature range, like for example skutterudites,[10] originates from the layered crystal structure, with phonons scattering at the interfaces between the conductive and insulating layers, and the presence of Bi which is an heavy element and is known to exhibit strong anharmonic vibrations that are detrimental for heat transfer.

The main limitation of undoped BiCuSeO for thermoelectric applications originates from its rather high electrical resistivity, of the order of 100 mΩ cm. The electrical conductivity can be improved by increasing the carriers' concentration through alkali metals, i.e., Mg, Ca, Sr, Ba doping, and Cu vacancies.[9,11–14] However, the hole mobility is strongly reduced by alkaline-earth doping, which limits the improvement of ZT. This decrease is probably linked to the very different electronic configuration of Bi^{3+} and A^{2+} with A being an alkaline-earth metal, and to the point defect scattering that originates from the large mass difference of Bi^{3+} and A^{2+}. Thus, a good path to overcome this limitation could be to find a new doping element with both similar mass and electronic configuration to that of Bi^{3+}.

In this work, we show that Pb^{2+} can substitute for Bi^{3+} and can also be used to optimize the charge carrier concentration, which results in improved TE properties as compared to undoped BiCuSeO. Moreover, the holes mobility is less reduced with Pb^{2+} doping as compared to alkaline-earth doping. However, the solubility limit of Pb^{2+} in this structure is too low to reach the optimum carriers concentration, which makes the thermoelectric performances of $Bi_{1-x}Pb_xCuSeO$ limited as compared to alkaline-earth doped BiCuSeO.

$Bi_{1-x}Pb_xCuSeO$ ($x = 0$, 0.01, 0.02, 0.03, 0.04, 0.05, 0.06, 0.07, and 0.2) samples were synthesized using an one step solid state reaction. Stoichiometric mixtures of Bi_2O_3 (BHO, 99.5%), Bi (Aldrich, 99.99%), Se (Alfa Aesar, 99.99%), Cu (Merck, 99.9%), and Pb (Alfa Aesar 99.5%) powders were grinded by hand using an agate mortar and pressed into pellets under uniaxial stress (250 MPa), then heated at 973 K for 12 h in silica tubes sealed under argon. The obtained samples were ground and subsequently densified by using a spark plasma sintering (SPS) system (SPS-511 S) at 948 K with holding time of 10 min in a ø = 15 mm graphite mold under an uniaxial compressive stress of 100 MPa in an argon atmosphere.

Room temperature X-ray diffraction (XRD) characterization was performed using a Panalytical X'Pert diffractometer by using a Cu Kα1 radiation obtained using a Ge(111) incident monochromator and an X'celerator detector. Rietveld refinement was performed to calculate the lattice constants of samples using FULLPROF software.[15] The specific heat C_p was measured using a Quantum Design physical properties measurement system (PPMS) from 300 K to 2 K. Hall measurements were performed in the PPMS environment from 300 K to 20 K using a Keithley 6220 current source and a Keithley 2182 A nanovoltmeter. The hall coefficient was obtained from the linear fit of the Hall resistivity between −9 T and 9 T. Seebeck coefficient S and electrical resistivity ρ were measured simultaneously by differential method with two T-type thermocouples by using the slope of V-T curve with gradients up to about 0.2 K/mm, by using a laboratory made system in a He-free cryostat from 20 K to

[a]Author to whom correspondence should be addressed. Electronic mail: greenspan513@163.com.

300 K. From 310 K to 873 K, Seebeck coefficient S and electrical resistivity ρ were measured simultaneously by the standard four-probe method using another laboratory made system in argon atmosphere.[16] All electrical characterizations were performed on bars cut from the pellets in a direction perpendicular to the pressing direction.

X-ray diffraction patterns at room-temperature for all the samples are shown in Fig. 1(a). It can be seen that for $Bi_{1-x}Pb_xCuSeO$ samples (with $x = 0$ to 0.07), the main diffraction peaks which are very sharp correspond to BiCuSeO (JCPD No. 45-0296) phase, no other phase being detected obviously from the XRD patterns (there are too many impurity phases corresponding to PbSe in XRD pattern of $Bi_{0.8}Pb_{0.2}CuSeO$ which are not shown in the figure). However, a small amount of $CuBi_2O_4$ phase was detected for the $Bi_{1-x}Pb_xCuSeO$ with $x = 0.07$, as exhibited in the figure. Accurate lattice parameters calculated from the XRD data using Rietveld refinement, shown in Fig. 1(b), indicate that lattice constants a and c slightly increase monotonically with increasing Pb content from 0.01 to 0.07 (see supplementary material at supplementary material 1 for Rietveld refinements of these XRD patterns).[22] Present results manifest that Pb has been introduced into BiCuSeO, leading to the formation of $Bi_{1-x}Pb_xCuSeO$ compounds with the solubility limit between 0.06 and 0.07. Indeed, the ionic radius of Pb^{2+} (1.29 Å) is larger than that of Bi^{3+} (1.17 Å) which results in a lattice expansion with increasing Pb content (as Pb^{2+} and Bi^{3+} are located in a distorted square antiprism environment, we have chosen to compare the ionic radii in a coordination number of viii as given by Shannon.)[17] At a first glance, compared with the larger solubility limit (0.35) of Sr^{2+} in $Bi_{1-x}Sr_xCuSeO$, the much smaller solubility limit of Pb^{2+} in $Bi_{1-x}Pb_xCuSeO$ may originate from the slightly larger ionic radius of Pb^{2+} than ionic radius of Sr^{2+} (1.26 Å). However, such a low solubility limit for Pb^{2+} was not expected as we had shown previously that the lattice can accommodate a large increase of both a and c, which reach 3.949 Å and 9.092 Å, respectively, in $Bi_{0.65}Sr_{0.35}CuSeO$,[18] much larger than the values observed in $Bi_{0.94}Pb_{0.06}CuSeO$. Moreover, contrary to the Sr-doped samples, no evolution with the Pb content of the $CuSe_4$ tetrahedral angles and of the Cu-Se distance have been observed, which shows that Pb^{2+} doping does not influence the local environment of Cu in the $[Cu_2Se_2]$ layer. Therefore, it seems that the low Pb^{2+} solubility limit cannot be explained using simple structural characteristics.

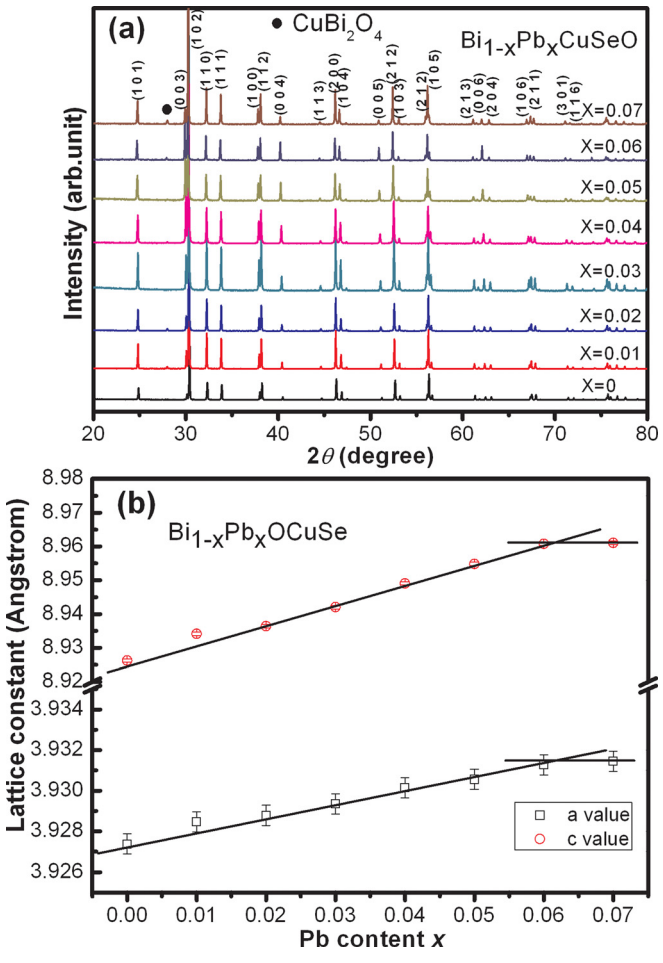

FIG. 1. (a) XRD patterns (CuK_α irradiation) of $Bi_{1-x}Pb_xCuSeO$ ($x = 0$, 0.01, 0.02, 0.03, 0.04, 0.05, 0.06, and 0.07) at R.T. (b) Composition (x) dependence of lattice parameters a and c for $Bi_{1-x}Pb_xCuSeO$ ($x = 0$, 0.01, 0.02, 0.03, 0.04, 0.05, 0.06, and 0.07) at R.T. Solid lines are guides for the eyes which help to determine the solution limit.

The temperature dependences of electrical resistivity and Seebeck coefficient for $Bi_{1-x}Pb_xCuSeO$ ($x = 0$ to 0.06) in the range of 25-300 K and 310-873 K are shown in Fig. 2. A good agreement can be observed between the low and high temperature measurements, using two distinct measurement devices. Enhanced electrical resistivity with increasing temperature from 50 to 300 K and the positive values of the Seebeck coefficient indicate a p-type degenerate semiconductor behavior from low temperature to high temperature for all doped samples. The electrical resistivity and Seebeck coefficient upturns observed for the undoped sample are consistent with our previous observations, but cannot be explained yet.[9] Moreover, the electrical resistivity and Seebeck coefficient of $Bi_{1-x}Pb_xCuSeO$ both decreased monotonically in all temperature range with increasing Pb content. For instance, at room temperature, the electrical resistivity and Seebeck coefficient decreased from 84.8 mΩ cm and 402.2 μV/K for pristine BiCuSeO to 2.3 mΩ cm and 99.7 μV/K for $Bi_{0.94}Pb_{0.06}CuSeO$, respectively. At 873 K, the electrical resistivity and Seebeck coefficient decreased from 63.5 mΩ cm and 373.6 μV/K for pristine BiCuSeO to 9.2 mΩ cm and 179.9 μV/K for $Bi_{0.94}Pb_{0.06}CuSeO$.

Combining the electrical resistivity and Seebeck coefficient, the calculated power factor ($PF = S^2/\rho$) in the range of 25-300 K and 310-873 K is shown in Fig. 2. The power factor of $Bi_{1-x}Pb_xCuSeO$ ($x = 0.03$) is 4.5 $\mu W\ cm^{-1}\ K^{-2}$ at 300 K and 5.3 $\mu W\ cm^{-1}\ K^{-2}$ at 873 K, which are both 2.4 times larger than pristine BiCuSeO at 300 K (1.9 $\mu W\ cm^{-1}\ K^{-2}$) and 873 K (2.2 $\mu W\ cm^{-1}\ K^{-2}$), respectively. It is noteworthy that the power factor does not increase monotonously with Pb^{2+} fraction, but reaches a maximum between x = 0.03 and x = 0.04. This maximum was not expected, as the power factor increases monotonously with Sr^{2+} and Ba^{2+} doping up to x = 0.1 and x = 0.075, respectively.[12,16] This difference can be explained by a smaller decrease of the hole mobility with Pb^{2+} doping as compared to Sr^{2+} or Ba^{2+} doping, see later.

Carriers concentration for $Bi_{1-x}Pb_xCuSeO$ ($x = 0$ to 0.06) has been calculated using measured Hall coefficients.

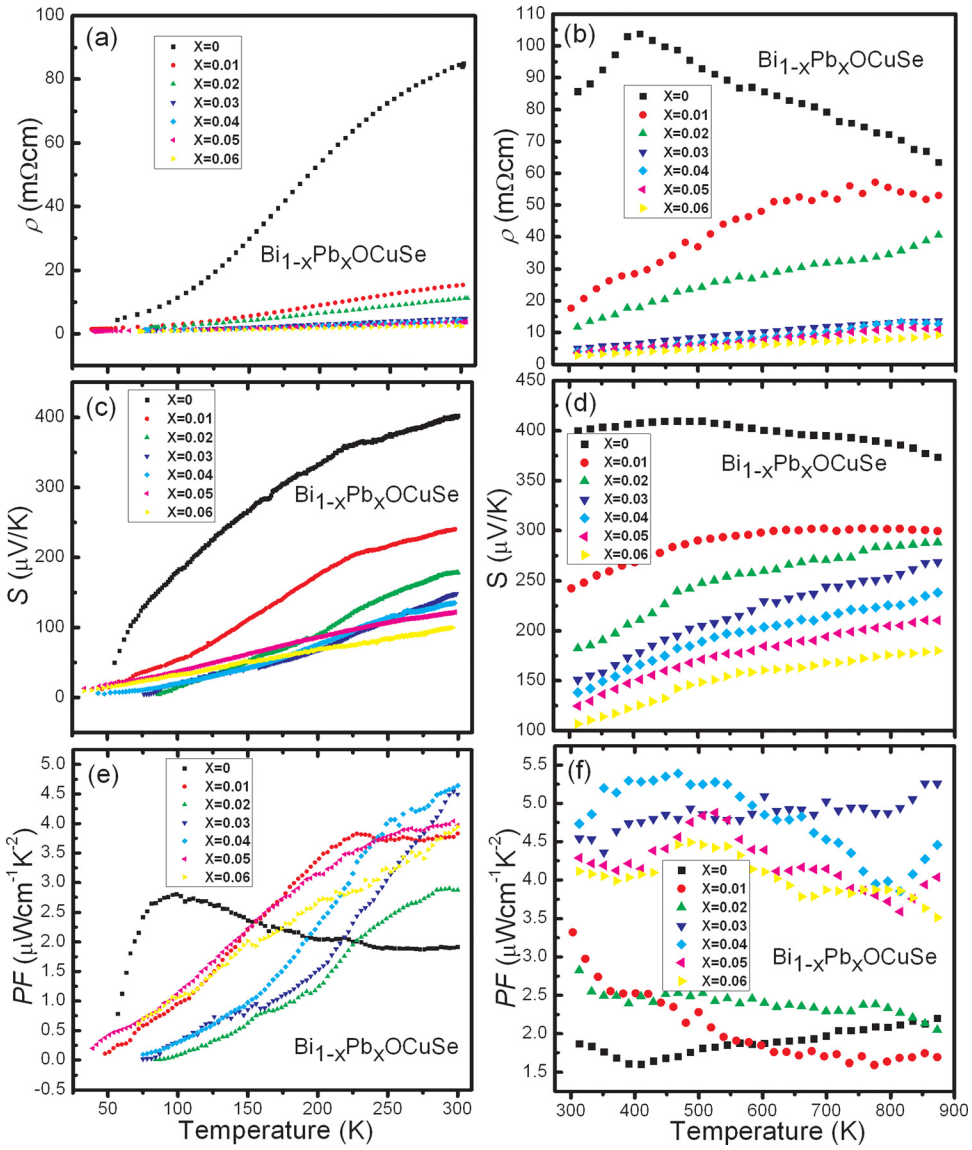

FIG. 2. Temperature dependence of the thermoelectric properties of the series $Bi_{1-x}Pb_xCuSeO$: (a) Electrical resistivity from 25 K to 310 K; (b) electrical resistivity from 310 K to 873 K; (c) Seebeck coefficient from 25 K to 310 K; (d) Seebeck coefficient from 310 K to 873 K; (e) power factor from 25 K to 310 K; (f) power factor from 310 K to 873 K.

With the increase of Pb content, the carrier concentration of $Bi_{1-x}Pb_xCuSeO$ increased monotonically from 6.6×10^{18} cm^{-3} for pristine BiCuSeO to 1.07×10^{21} cm^{-3} for $Bi_{0.94}Pb_{0.06}CuSeO$ at room temperature as shown in Table I. Since dopant Pb has the electronic structure $[Xe]4f^{14}5d^{10}6s^26p^2$, the substitution of Pb for Bi ($[Xe]4f^{14}5d^{10}6s^26p^3$) will introduce acceptor levels in the band gap of the host, resulting in an increase in the hole concentration. A very good agreement has been observed between the calculated holes concentrations and the one obtained from the nominal Pb^{2+} concentration assuming that each Pb^{2+} induces one free hole in the valence band, which shows a very good doping efficiency of Pb^{2+}, as compared for example to Mg^{2+}.[11] As expected, the increase of carriers concentration is connected to a rapid decrease of the holes mobility, which falls below 3 cm^2 V^{-1} s^{-1} for a Pb^{2+} fraction as low as x = 0.02 (Table I). However, these values are higher than the one observed in Sr^{2+} or Ba^{2+} doped BiCuSeO, which falls below 2 cm^2 V^{-1} s^{-1}.[18] This

TABLE I. Carrier concentration [n] and holes mobility μ at room temperature, the Sommerfeld coefficient γ, the coefficient of the Debye T^3 lattice heat capacity β, the Debye temperature Θ_D from heat capacity measurements at low temperature, the density of states at the Fermi energy $D(E_F)$ for $Bi_{1-x}Pb_xCuSeO$ ($x = 0$ to 0.06).

$Bi_{1-x}Pb_xCuSeO$	[n] (10^{20} cm^{-3})	μ (cm^2 V^{-1} s^{-1})	γ (mJ mol^{-1} K^{-2})	β (mJ mol^{-1} K^{-4})	Θ_D (K)	$D(E_F)$ (states/erg.f.u.)
$x = 0$	0.066	11.2	0.113	0.525	245	0.05
$x = 0.01$	1.24	3.3	0.906	0.533	244	0.39
$x = 0.02$	2.66	2.1	1.57	0.512	247	0.67
$x = 0.03$	4.27	3.0	2.56	0.521	246	1.1
$x = 0.04$	6.45	2.4	3.67	0.520	246	1.6
$x = 0.05$	8.39	2.0	4.93	0.522	246	2.1
$x = 0.06$	10.7	2.3	5.57	0.544	243	2.4

difference can probably be explained by the smaller influence of Pb^{2+} doping on the local structure of the $[Cu_2Se_2]$ layer as compared to Sr^{2+} and Ba^{2+}, and to smaller point defect scattering. Due to the larger mobility of Pb^{2+} doped samples, the carriers concentration required to reach a low electrical resistivity is lower, which shifts the improvement of the power factor to lower doping fractions. However, due to the low solubility limit of Pb^{2+}, it was not possible to increase the carrier concentration in order to reach power factor values larger than the ones observed in alkaline-earth doped BiCuSeO.

Fig. 3(a) shows the temperature dependence of the holes mobility of $Bi_{0.95}Pb_{0.05}CuSeO$, which is characteristic of the other samples of the series. Above 150 K, the temperature dependence can be well fitted using a power law $\mu \approx T^{\lambda}$ with $\lambda = -1.2$. This value is intermediate between $\lambda = -3/2$ and $\lambda = -1$ which correspond to a carriers scattering by acoustic phonons for non-degenerate semiconductors and degenerate semiconductors, respectively. Therefore, it can be reasonably assumed that acoustic phonons scattering is the main scattering process in the $Bi_{1-x}Pb_xCuSeO$ at least above 150 K.

There are several factors that could influence the Seebeck coefficient, carrier concentration n, scattering factor λ, and the carrier effective mass m^* according to the following relations derived from the Boltzmann transport equations, assuming parabolic band structure in the relaxation time approximation[19,20]

$$m^* = \frac{h^2}{2k_BT}\left[\frac{n}{4\pi F_{1/2}(\eta)}\right]^{2/3}, \tag{1}$$

$$S = \pm\frac{k_B}{e}\left(\frac{(\lambda+5/2)F_{\lambda+3/2}(\eta)}{(\lambda+3/2)F_{\lambda+1/2}(\eta)} - \eta\right), \tag{2}$$

$$F_n(\eta) = \int_0^\infty \frac{\chi^n}{1+e^{\chi-\eta}}d\chi. \tag{3}$$

Here, h is Planck's constant (Js), k_B is Boltzmann's constant (J/K), T is the absolute temperature, $\eta = E_F/(k_BT)$ is the reduced Fermi energy, e is the electronic charge (C), and $F_n(\eta)$ is the n-th order Fermi integral, which is always positive and increases with η and n.

It is then seen that as η is increased, this yields an increase of n and a decrease of the absolute Seebeck coefficient $|S|$. Such a contrary relationship then dictates an optimal value for η for maximizing the power factor, S^2/ρ. In addition, increasing m^* or λ would also increase $|S|$.[19] These results indicate that decreasing resistivity and Seebeck coefficient of $Bi_{1-x}Pb_xCuSeO$ with increasing Pb content mainly originated from the increasing carrier concentration.

The heat capacity C_p of BiCuSeO as a function of temperature from 2 K to 293 K is presented in Fig. 3(b). The heat capacity of undoped BiCuSeO attains a value of 99.5 J/mol K at room temperature which is exactly the same as the expected classical high-T Dulong-Petit lattice heat capacity value $C_p = 3nR = 12\,R = 99.8$ J/mol K at constant volume V, where R is the molar gas constant, and n = 4 is the number of atoms per formula unit (f.u.) of BiCuSeO. The inset in Fig. 3(b) shows the low-T data of BiCuSeO plotted as C_p/T versus T^2 allowing a conventional fit by

$$\frac{C_p(T)}{T} = \gamma + \beta T^2. \tag{4}$$

Here, γ is the Sommerfeld electronic linear specific heat coefficient and β is the coefficient of the Debye T^3 lattice heat capacity at low temperature which obtained by linear fit of the data below 3.5 K according to Eq. (4). γ increases monotonically from 113 μJ mol^{-1} K^{-2} for pristine BiCuSeO to 5.57 mJ mol^{-1} K^{-2} for $Bi_{0.94}Pb_{0.06}CuSeO$ with increasing Pb content as shown in Table I. However, β is nearly a constant, the variable range is between 0.51 mJ mol^{-1} K^{-4} and 0.54 mJ mol^{-1} K^{-4} which may originate to measurement error (Table I).

We obtained the value of the Debye temperature Θ_D of $Bi_{1-x}Pb_xCuSeO$ ($x = 0$ to 0.06) from β using the relation $\Theta_D = \left(\frac{12\pi^4 N_A k_B n}{5\beta}\right)^{1/3}$, where N_A is Avogadro's number and k_B is Boltzmann's constant, yielding Θ_D of $Bi_{1-x}Pb_xCuSeO$ ($x = 0$ to 0.06) around 245 K (Table I). The results show that Pb doping does not change the Debye temperature of BiCuSeO. Indeed Pb^{2+} doping, with small concentrations, were not expected to influence strongly the phonon spectra of this material. The Sommerfeld coefficient γ can be used to estimate the density of states at the Fermi level $D(E_F)$ for both spin directions according to[21]

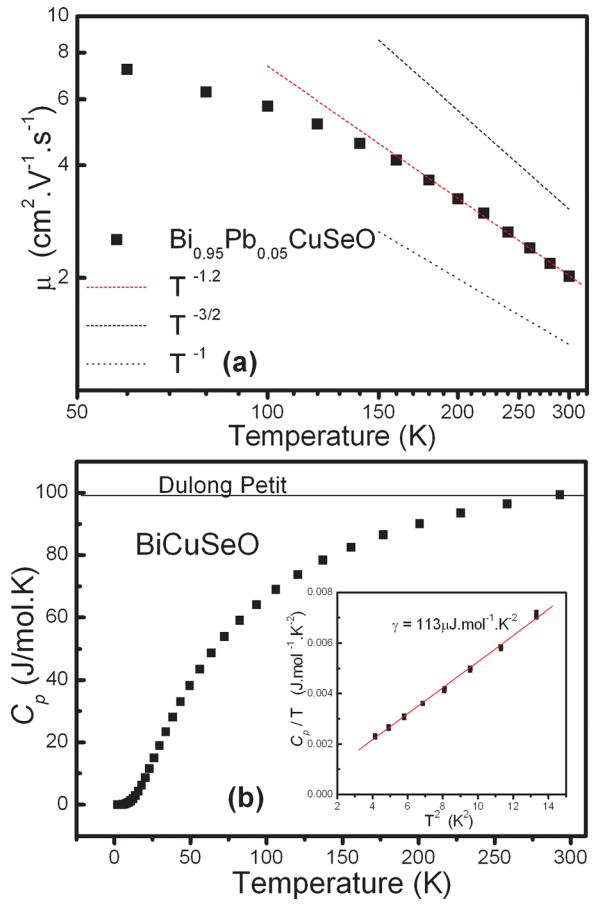

FIG. 3. (a) Temperature dependence of the holes mobility of $Bi_{0.95}Pb_{0.05}CuSeO$ (which is characteristic of all the samples in the series). The dotted red line is the best fit of the mobility behaviour above 150 K using a power law, and the black dotted lines indicate a $T^{-3/2}$ and T^{-1} behaviour. (b) The heat capacity C_p of BiCuSeO as a function of temperature from 2 K to 293 K. The inset in (b) is the low-T data of BiCuSeO plotted as C_p/T versus T^2 allowing a conventional fit by $\frac{C_p(T)}{T} = \gamma + \beta T^2$.

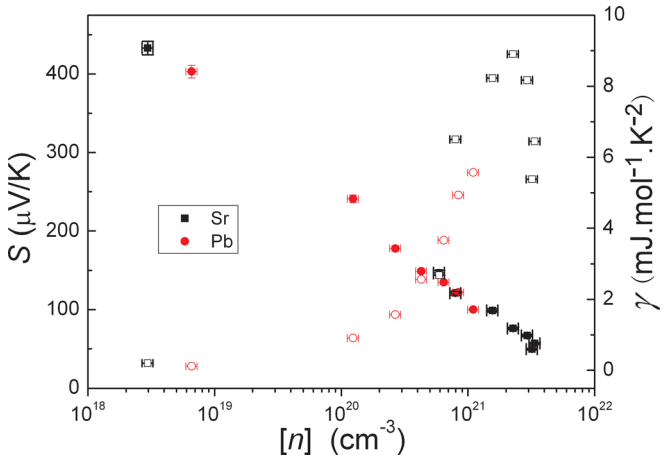

FIG. 4. Seebeck coefficient S and Sommerfeld coefficient γ as a function of carrier concentration modified by Pb and Sr doping.

$$\gamma = \frac{\pi^2 {k_B}^2}{3} D(E_F)(1 + \lambda_{e-ph}), \tag{5}$$

where $\lambda_{\text{e-ph}}$ is the electron-phonon coupling constant, which we set to zero. The obtained values of $Bi_{1-x}Pb_xCuSeO$ ($x = 0$ to 0.06) for both spin directions are shown in Table I. The magnitude of $D(E_F)$ increases monotonically with increasing Pb content. This result is consistent with the ones we obtained previously in the $Bi_{1-x}Sr_xCuSeO$ series, which showed that the density of states increases up to $Sr = 0.2$ where it starts to decrease, in agreement with the band structure calculations.[18]

Now, we compare the effects on the TE properties of Pb and Sr doping. Fig. 4 shows Seebeck coefficient and Sommerfeld coefficient γ as a function of carrier concentration, with both Pb and Sr doping. One can see that the carriers concentration dependence of both Seebeck coefficient and Sommerfeld coefficient γ match very well between Pb and Sr doping. Therefore, it seems that despite their very different electronic configurations, Pb^{2+} and Sr^{2+} have a very similar influence on the electronic properties of BiCuSeO, which confirms that the doping in this system can be reasonably well described by a shift of the Fermi level within a rigid band model framework. However, we have seen that the holes mobility is slightly improved with Pb^{2+} doping as compared to Sr^{2+} or Ba^{2+}, probably owing to a reduced point defect scattering and a smaller $[Cu_2Se_2]$ disorder due to the similar atomic mass and electronic configuration of Pb^{2+} and Bi^{3+}. Therefore, although the solubility limit of Pb^{2+} in BiCuSeO is too low to reach the optimum carriers concentration, this result demonstrates the effectiveness of our approach toward the improvement of the thermoelectric properties of this system.

In summary, the electrical transport properties of p-type $Bi_{1-x}Pb_xCuSeO$ ($x = 0$ to 0.06) are improved by Pb^{2+} doping due to the increased carriers concentration, and the power factor of $Bi_{0.97}Pb_{0.03}CuSeO$ reaches 5.3 μW cm^{-1} K^{-2} at 873 K which is around 2.4 times larger than undoped BiCuSeO. The influence of Pb^{2+} doping on the electronic structure is the same as the one obtained with Sr^{2+}, and the system can be described in a rigid band model framework. The atomic mass and electronic configuration of Pb^{2+} being very similar to that of Bi^{3+}, the decrease of the holes mobility is reduced as compared to Sr^{2+} doping, which could be beneficial to the thermoelectric performances. However, although this approach seemed promising, the low solubility limit of Pb^{2+} in BiCuSeO prevented us from further improving the power factor of this system compared to alkaline-earth doping.

This work was supported by the ANR through the project OTHer (ANR 2011 JS08 012 01).

[1]F. J. DiSalvo, Science **285**, 703 (1999).
[2]G. J. Snyder and E. S. Toberer, Nature Mater. **7**, 105 (2008).
[3]Y. Masuda, D. Nagahama, H. Itahara, T. Tani, W. S. Seoc, and K. Koumotoa, J. Mater. Chem. **13**, 1094 (2003).
[4]S. Ohta, T. Nomura, H. Ohta, M. Hirano, H. Hosono, and K. Koumoto, Appl. Phys. Lett. **87**, 092108 (2005).
[5]M. Ohtaki, T. Tsubota, K. Eguchi, and H. Arai, J. Appl. Phys. **79**, 1816 (1996).
[6]D. Bérardan, E. Guilmeau, A. Maignan, and B. Raveau, Solid State Commun. **146**, 97 (2008).
[7]E. Guilmeau, D. Bérardan, C. Simon, A. Maignan, B. Raveau, D. Ovono Ovono, and F. Delorme, J. Appl. Phys. **106**, 053715 (2009).
[8]A. M. Kusainova, P. S. Berdonosov, L. G. Akselrud, L. N. Kholodkovskaya, V. A. Dolgikh, and B. A. Popovkin, J. Solid State Chem. **112**, 189 (1994).
[9]L. D. Zhao, D. Berardan, Y. L. Pei, C. Byl, L. Pinsard-Gaudart, and N. Dragoe, Appl. Phys. Lett. **97**, 092118 (2010).
[10]X. Tang, H. Li, Q. Zhang, M. Niino, and T. Goto, J. Appl. Phys. **100**, 123702 (2006).
[11]J. Li, J. H. Sui, Y. L. Pei, C. Barreteau, D. Berardan, N. Dragoe, W. Cai, and L. D. Zhao, J. Alloys Compd. **551**, 649 (2013).
[12]Y. L. Pei, F. Li, J.-F. Li, Q. J. Liu, W. Pan, C. Barreteau, D. Berardan, N. Dragoe, J. Q. He, and L. D. Zhao, "High thermoelectric performance of Ca doped BiCuSeO system benefits from intrinsically low thermal conductivity," J. Am. Chem. Soc. (submitted).
[13]J. Li, J. H. Sui, Y. L. Pei, C. Barreteau, D. Berardan, N. Dragoe, W. Cai, J. Q. He, and L. D. Zhao, Energy Environ. Sci. **5**, 8543 (2012).
[14]Y. Liu, L. D. Zhao, Y. C. Liu, J. L. Lan, W. Xu, F. Li, B. P. Zhang, D. Berardan, N. Dragoe, Y. H. Lin, C. W. Nan, J. F. Li, and H. M. Zhu, J. Am. Chem. Soc. **133**, 20112 (2011).
[15]J. Rodriguez-Carvajal, Physica B **192**, 55 (1993).
[16]C. Byl, D. Berardan, and N. Dragoe, Meas. Sci. Technol. **23**, 035603 (2012).
[17]R. D. Shannon, Acta Crystallogr. **32**, 751 (1976).
[18]C. Barreteau, D. Berardan, E. Amzallag, L. D. Zhao, and N. Dragoe, Chem. Mater. **24**, 3168 (2012).
[19]P. Pichanusakorn and P. Bandaru, Appl. Phys. Lett. **94**, 223108 (2009).
[20]P. Pichanusakorn and P. Bandaru, J. Appl. Phys. **107**, 074304 (2010).
[21]C. Kittel, *Introduction to Solid State Physics*, 8th ed. (Wiley, New York, 2005).
[22]See supplementary material at http://dx.doi.org/10.1063/1.4775593 for Rietveld refinement results of Pb doped BiCuSeO XRD patterns.